

Cusp-like structure in the $\gamma p \rightarrow K^+ \Sigma^0$ cross section at low momentum transfer

T.C. Jude,^{1,*} S. Alef,¹ P. Bauer,¹ D. Bayadilov,^{2,3} R. Beck,² A. Bella,^{1,†} J. Bieling,^{2,†} A. Braghieri,⁴ P.L. Cole,⁵ D. Elsner,¹ R. Di Salvo,⁶ A. Fantini,^{6,7} O. Freyermuth,¹ F. Frommberger,¹ F. Ghio,^{8,9} S. Goertz,¹ A. Gridnev,³ D. Hammann,^{1,†} J. Hannappel,¹ K. Kohl,¹ N. Kozlenko,³ A. Lapik,¹⁰ P. Levi Sandri,¹¹ V. Lisin,¹⁰ G. Mandaglio,^{12,13} F. Messi,^{1,†} R. Messi,^{6,7} D. Moricciani,⁶ V.A. Nikonov,^{2,3,‡} V. Nedorezov,¹⁰ D. Novinskiy,³ P. Pedroni,⁴ A. Polonskiy,¹⁰ B.-E. Reitz,^{1,†} M. Romaniuk,^{6,14} A.V. Sarantsev,^{2,3} G. Scheluchin,¹ H. Schmieden,¹ A. Stugelev,³ V. Sumachev,^{3,‡} V. Vugna,^{1,†} V. Tarakanov,³ and T. Zimmermann^{1,†}

(The BGOOD Collaboration)

¹*Rheinische Friedrich-Wilhelms-Universität Bonn,
Physikalisches Institut, Nußallee 12, 53115 Bonn, Germany*

²*Rheinische Friedrich-Wilhelms-Universität Bonn,
Helmholtz-Institut für Strahlen- und Kernphysik, Nußallee 14-16, 53115 Bonn, Germany*

³*Petersburg Nuclear Physics Institute, Gatchina, Leningrad District, 188300, Russia*

⁴*INFN sezione di Pavia, Via Agostino Bassi, 6 - 27100 Pavia, Italy*

⁵*Lamar University, Department of Physics, Beaumont, Texas, 77710, USA*

⁶*INFN Roma “Tor Vergata”, Via della Ricerca Scientifica 1, 00133, Rome, Italy*

⁷*Università di Roma “Tor Vergata”, Dipartimento di Fisica,
Via della Ricerca Scientifica 1, 00133, Rome, Italy*

⁸*INFN sezione di Roma La Sapienza, P.le Aldo Moro 2, 00185, Rome, Italy*

⁹*Istituto Superiore di Sanità, Viale Regina Elena 299, 00161, Rome, Italy*

¹⁰*Russian Academy of Sciences Institute for Nuclear Research,
Prospekt 60-letiya Oktyabrya 7a, 117312, Moscow, Russia*

¹¹*INFN - Laboratori Nazionali di Frascati, Via E. Fermi 54, 00044, Frascati, Italy*

¹²*INFN sezione Catania, 95129, Catania, Italy*

¹³*Università degli Studi di Messina, Dipartimento MIFT,
Via F. S. D’Alcontres 31, 98166, Messina, Italy*

¹⁴*Institute for Nuclear Research of NASU, 03028, Kyiv, Ukraine*

Differential cross section data for $\gamma p \rightarrow K^+ \Sigma^0$ has been measured at the BGOOD experiment for extremely forward angles. A three quarter drop in strength over a narrow range in energy and strong dependence on polar angle is observed at a centre of mass energy of 1900 MeV. Residing close to multiple open and hidden strangeness thresholds, the kinematics are consistent with threshold effects and exotic structure which may contribute to the reaction mechanism.

PACS numbers: 13.60.Le, 25.20.-x

Recent discoveries of exotic “multi-quark” hadronic states which are inadequately described as constituent three and two valence quark systems, has challenged our understanding of the degrees of freedom afforded in QCD. This includes for example, in the charmed sector, P_c states at LHCb [1], XYZ mesons at numerous facilities [2] and in the light ud sector, the $d^*(2380)$ at COSY [3]. Descriptions of multi-quark states have existed however since the conception of quark models [4–6], and due to the proximity of the chiral symmetry breaking scale to the nucleon mass, it is possible that light mesons interact as elementary objects, giving rise to molecular systems and meson re-scattering effects near thresholds [7, 8]. Indeed, models including meson-baryon interactions and dynamically generated states [9–14] have had improved success in describing nucleon excitation spectra. In the strangeness sector, such states [15–17] may have been observed in

$K^0 \Sigma^+$ photoproduction at the K^*Y thresholds [18–20], where equivalent models [21] were able to describe the $P_C(4450)$ and $P_C(4380)$ states. The $\Lambda(1405)$ is also considered a molecular $\bar{K}N$ state to some extent [14], which is also supported by Lattice QCD calculations [22].

The study of extended, loosely bound systems derived from meson-baryon interactions requires minimal momentum transfer kinematics. For fixed target photoproduction experiments, access to forward meson angles is therefore crucial. This letter presents forward angle $\gamma p \rightarrow K^+ \Sigma^0$ cross sections measured at the BGOOD experiment [23] at the ELSA electron accelerator facility [24, 25]. A strong cusp-like drop in strength is observed at extremely forward angles at a centre of mass energy of 1900 MeV. The kinematics and close lying thresholds may be indicative of exotic structure manifest in the reaction mechanism.

BGOOD is composed of a *Forward Spectrometer* for charged particle identification over laboratory frame polar angles 1° to 12° . This is complemented by the *BGO Rugby Ball*, an almost 4π central calorimeter ideal for photon detection with sub-detectors for charged particle identification. The experimental conditions and K^+

* Corresponding author: jude@physik.uni-bonn.de

† No longer employed in academia

‡ Deceased

identification are described in refs. [23, 26].

The data were taken over 22 days using an electron beam energy of 3.2 GeV and a 6 cm long liquid hydrogen target. The electron beam was incident upon a thin crystalline radiator to produce an energy tagged bremsstrahlung photon beam which was subsequently collimated. The photon beam energy, E_γ , was determined per event by momentum analysing the post bremsstrahlung electrons in the *Photon Tagger*. K^+ were identified in the Forward Spectrometer via momentum and β determination. The photon from the decay $\Sigma^0 \rightarrow \Lambda\gamma$ (labelled γ' herein) was required to be identified in the BGO Rugby Ball. Photons were rejected as γ' candidates if the invariant mass of combinations of two photons was consistent with the π^0 mass. The missing mass to the $K^+\gamma'$ system was determined for remaining γ' candidates and the photon where this was the closest to the Λ mass was identified. The four momentum of the γ' was then boosted into the rest frame of the Σ^0 . Figure 1 shows the γ' energy in this frame, where the peak at 74 MeV is consistent with the expected two body decay momentum. Background is predominantly from misidentified photons and neutrons from $K^+\Lambda$, and other hadronic interactions where π^+ are misidentified as K^+ . Two datasets were obtained, applying either a one or two sigma selection over the peak (69 to 79 MeV or 62 to 86 MeV respectively).

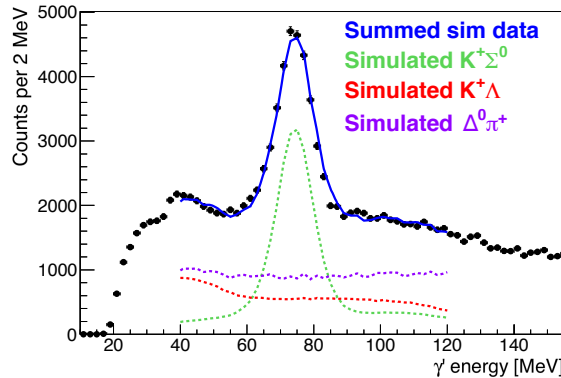


FIG. 1. γ' energy in the Σ^0 rest frame, with a peak consistent with the expected energy from the $\Sigma^0 \rightarrow \Lambda\gamma$ decay. Simulated spectra from $K^+\Sigma^0$, $K^+\Lambda$ and $\Delta^0\pi^+$ are fitted to the data.

The remaining candidate events were rejected if charged and neutral particle multiplicities exceeded either decay modes: $\Sigma^0 \rightarrow \gamma\Lambda \rightarrow \gamma(\pi^0 n)$ or $\gamma(\pi^- p)$.

The missing mass recoiling from forward K^+ , after the γ' identification is shown in Fig. 2. A fit was made using spectra from simulated $K^+\Lambda$, $K^+\Sigma^0$ and $K^+\Sigma^0(1385)$ events. Simulated $K^+\Lambda(1405)$ events were not included due to the mass degeneracy to the $\Sigma^0(1385)$. An additional combined e^+ and π^+ background was also included in the fit. The e^+ are from pair production in the beam in random coincidence with hardware triggers and the π^+ from other hadronic reactions. These distributions were generated by an equivalent analysis identifying negatively charged particles, where the e^- and π^- distributions are

the same. The 1σ γ' selection gave a lower yield of events, however an improved signal to background ratio. For the 2σ γ' selection above $E_\gamma = 1530, the integral of the background exceeded the signal. To avoid additional systematic errors, the 2σ data was used below 1530 MeV, and the 1σ data above. The detection efficiency shown in fig. 3 was determined using Geant4 [27]. This includes the loss of approximately 50% K^+ decaying mid-flight.$

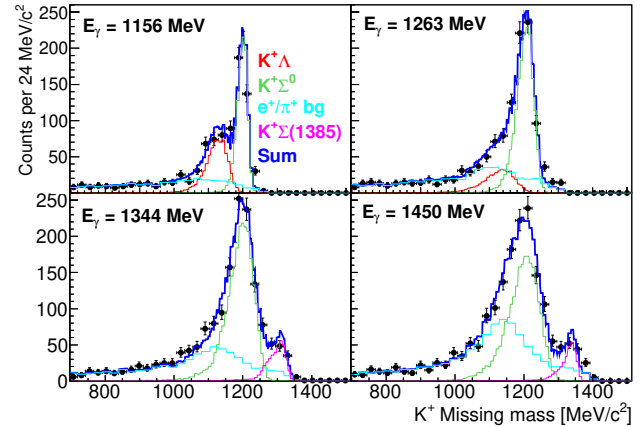


FIG. 2. Missing mass recoiling from forward K^+ candidates after a 2σ γ' identification for different labelled E_γ . The spectra are fitted with simulated $K^+\Lambda$, $K^+\Sigma^0$, $K^+\Sigma^0(1385)$, and e^+/π^+ background (red, green, magenta and cyan lines respectively, labelled in the top left panel). The blue line is the summed total fit.

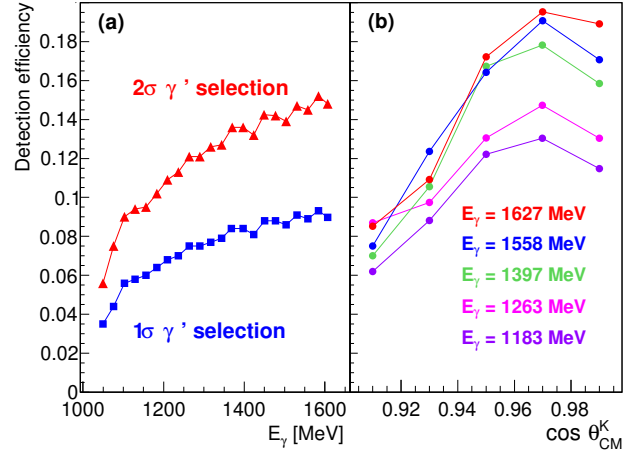


FIG. 3. Detection efficiency for: (a) $\cos \theta_{CM}^K > 0.9$ versus E_γ using either the 1σ or 2σ γ' selection (red triangles and blue squares respectively). (b) Versus $\cos \theta_{CM}^K$ for selected photon energy intervals for the 2σ γ' selection (labelled inset in descending order of both beam energy and detection efficiency). The connecting lines are an aid to guide the eye. Colour online.

Systematic uncertainties are the same as described in ref. [26] and are divided into two components. The *scaling*

uncertainty is a constant fraction of the measured cross section. The dominant sources of this are the photon beam spot position and the photon flux normalisation, both estimated as 4 %. The uncertainty in the γ' identification was determined by comparing the differential cross section for both the 1σ and 2σ γ' selection, shown in Fig. 4. The *fitting uncertainty* arises from extracting the number of events from the missing mass spectra and permits the individual movement of data points. This was determined by additionally including simulated $\Delta^0\pi^+$ events in the background distribution. A steeply rising uncertainty towards higher energies was determined, with approximately 4 %, 8 % and 28 % at $E_\gamma = 1400$, 1500 and 1600 MeV respectively.

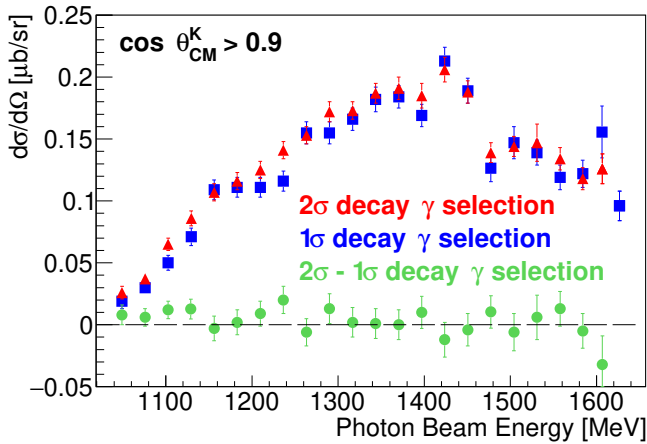


FIG. 4. Differential cross section for $\cos \theta_{\text{CM}}^K > 0.9$ using either the 1σ or 2σ γ' selection (red triangles and blue squares respectively). The green circles are the difference.

The $K^+\Sigma^0$ differential cross section for $\cos \theta_{\text{CM}}^K > 0.9$ is shown in fig. 5. Our new data provide the highest statistics from threshold to $W = 1970$ MeV, enabling a discrimination between conflicting previous datasets. There is generally good agreement to the CLAS data of Bradford [28], whereas the CLAS data of Dey [29] appears higher by approximately 20 % and the SAPHIR data of Glander [30] somewhat lower. Figures 6 and 7 show the differential cross section in $0.02 \cos \theta_{\text{CM}}^K$ intervals versus $\cos \theta_{\text{CM}}^K$ and W respectively. The drop at $W = 1900$ MeV is consistent with previous data sets, where it was regarded as a peak-like structure. Numerous PWA and isobar model solutions attributed this to $D_{13}(1895)$, $S_{31}(1900)$, $P_{31}(1910)$ and $P_{13}(1900)$ [31–34] for example, but with no firm agreement. The statistics and $\cos \theta_{\text{CM}}^K$ resolution of this data allow a “cusp-like” structure to be resolved at this energy, that was difficult to confirm prior. As is shown in fig. 7, this cusp-like structure becomes more pronounced at the most forward angle interval, $\cos \theta_{\text{CM}}^K > 0.98$, where there is a reduction of approximately 70 % over a 30 MeV range. At the most backward intervals, the cusp is difficult to discern, starting to only become visible around $0.94 < \cos \theta_{\text{CM}}^K < 0.96$.

The Bonn-Gatchina BG2019 solution [35], which is

largely constrained by the CLAS data, gives a reduced χ^2 of 6.03 when compared to this data (the cyan line in figs. 5, 7 and 6). After including this data and optimisations, a notable improvement of the reduced χ^2 to 2.08 was achieved (the magenta line), with no significant changes to the fit occurring at more backward $\cos \theta_{\text{CM}}^K$ covered by the CLAS data, as can be seen in fig. 6. Additional resonant contributions were iteratively included to test for further improvements. A $\Delta(1917)$ with $J = 5/2^-$ and a relatively narrow width of 59 MeV gave the best improvement to this data (not shown in the figures), however only influencing the most forward data points. The fit to the CLAS data was not significantly affected and this state has not been observed elsewhere. This is by no means settled however, and other factors could mimic this contribution. Further measurements, including single and double polarisation observables and analysis of other channels are required for a firm statement on including this resonance. The significant changes to the PWA solution however, given the comparatively small range of kinematics of this data, demonstrate the importance of forward angle coverage. The high angular resolution ensures that this data is particularly sensitive to high spin resonances due to contributing Legendre polynomials changing very quickly with respect to $\cos \theta_{\text{CM}}^K$ at forward angles. In associated strangeness photoproduction, which has often been used to search for unobserved “missing resonances”, in contrast to $K^+\Lambda$, s -channel Δ states can also contribute to $K\Sigma$.

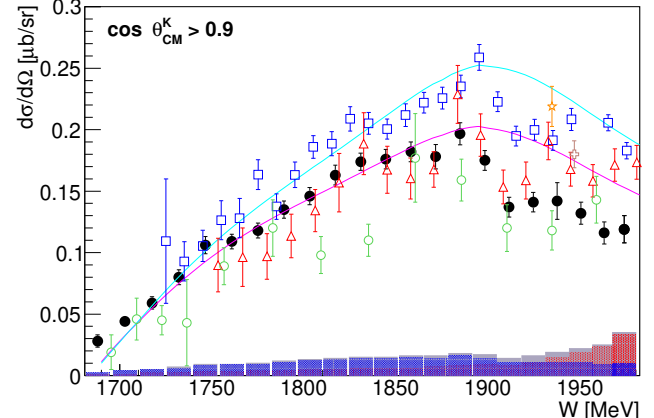


FIG. 5. $\gamma p \rightarrow K^+\Sigma^0$ differential cross section for $\cos \theta_{\text{CM}}^K > 0.90$ (black circles). The systematic uncertainties on the abscissa are in three components: The shaded blue, red and grey bars are the scaling, fitting and summed uncertainties respectively. Previous data of Dey *et al.* (CLAS) [29] (blue open squares), Bradford *et al.* (CLAS) [28] (red open triangles), Glander *et al.* (SAPHIR) [30] (green open diamonds), Sumihama *et al.* (LEPS) (orange open stars) [36] and Shiu *et al.* (LEPS) [37] (peach open crosses) are additionally shown. The Bonn-Gatchina PWA solutions [35] with and without the inclusion of the new data are the magenta and cyan lines respectively.

If an observed effect was derived from loosely bound

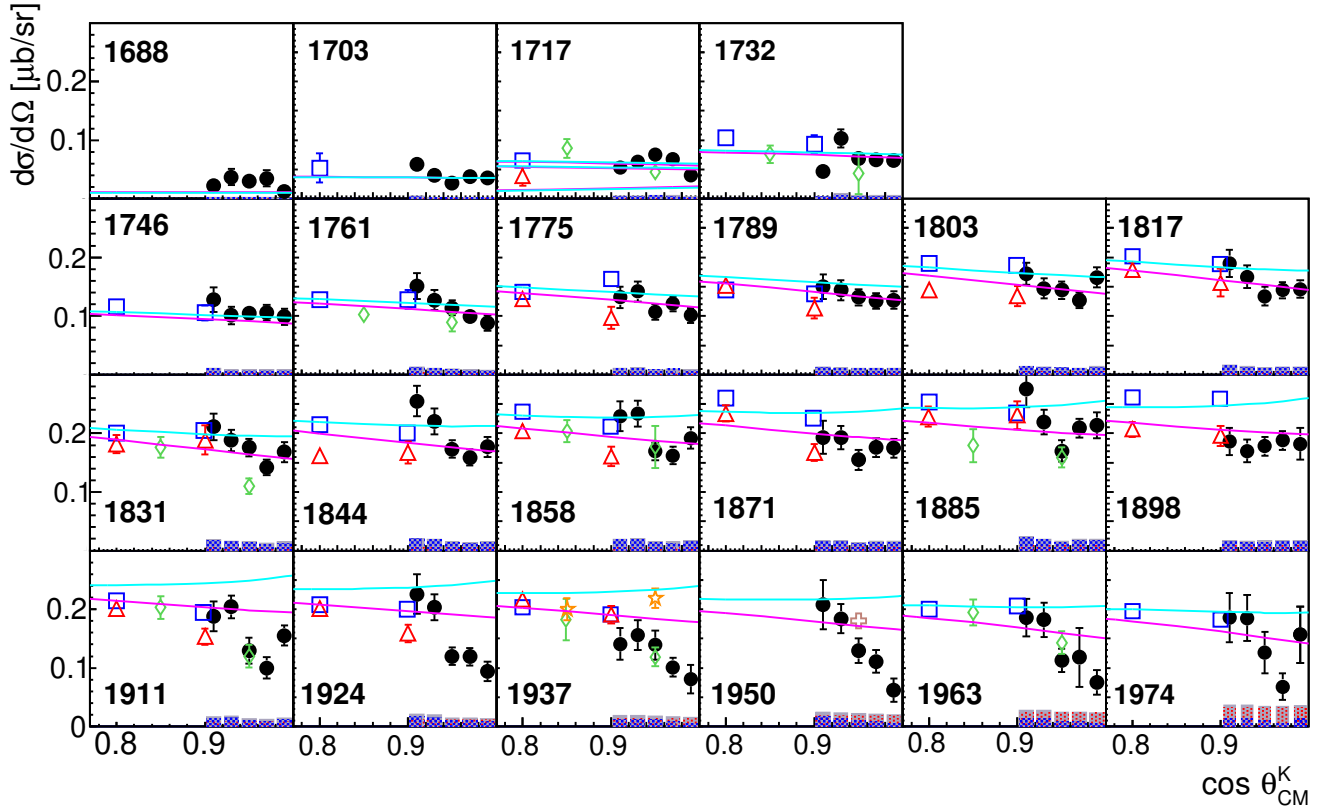


FIG. 6. Differential cross section versus $\cos \theta_{\text{CM}}^K$ in intervals of $0.02 \cos \theta_{\text{CM}}^K$ for each W interval labelled inset in MeV. The labelling of data points and fits are the same as in fig. 5.

structures, for example meson-baryon type multi-quark configurations, then momentum transfer would be crucial in t -channel production processes. Due to the relatively large size of such objects, their formation should be strongly suppressed if the momentum transfer significantly exceeds the typical Fermi momenta in nuclei, which is of the order of a few hundred MeV/c. The opposite would be true at low momentum transfer and small meson production angles, where an enhancement would be expected with a maximum at the minimum possible momentum transfer, t_{\min} , where the meson has a polar angle of 0° . In addition, such structures may be associated with anomalies in the t dependence of the production process at small t at the order of 0.05 GeV^2 . To investigate this, the Mandelstam variable, t , was determined for each W and $\cos \theta_{\text{CM}}^K$ interval. Examples are shown in fig. 8 and fitted with the function in eq. 1.

$$\frac{d\sigma}{dt} = \frac{d\sigma}{dt} \Big|_{t=t_{\min}} e^{S|t-t_{\min}|} \quad (1)$$

The differential cross section with respect to t at t_{\min} shown in fig. 9(a) indeed exhibits a particularly pronounced drop in strength at $W = 1900 \text{ MeV}$. It is interesting to observe the slope parameter, S , in fig. 9(b). S is positive and appears flat (although with limited statistics) for approximately the first 150 MeV from threshold, indicative of s -channel contributions. The fact that this

is over a larger W range compared to $K^+\Lambda$ shown in ref. [26] may be due to both N^* and Δ^* resonance contributions. At the cusp-like structure observed in fig. 9(a) an anomaly develops in the slope parameter S , where it drops at approximately 1840 MeV and turns negative, as would be expected for a dominantly t -channel process. This is further corroborated by inspecting the cross section as a function of three-momentum transfer from the photon to the recoiling baryon, q , shown in fig. 10. If the process is dominated by the recoil momentum the baryonic system is able to take, the cross section would be expected to “scale” with q , with a much weaker dependence on W . While it is clear by eye that there is a W dependence in fig. 10, this seems to vanish in the vicinity of the cusp-like structure, which can be evidenced in fig. 10(b) at $q \approx 0.54 \text{ GeV}/c$.

At the cusp-like structure at 1900 MeV , there is a sharp rise back to positive values of S , which then remains flat. This quick change with respect to W may indicate that a significant t -channel contribution is lost and could be interpreted as a threshold effect, where an off-shell contribution is produced on-shell above $W = 1900 \text{ MeV}$.

This strong dependence on angle, and therefore momentum exchange may suggest threshold dynamics or meson-baryon interactions playing a significant role in the reaction mechanism. The PWA extraction of quantum numbers, mass and width of the suggested Δ does

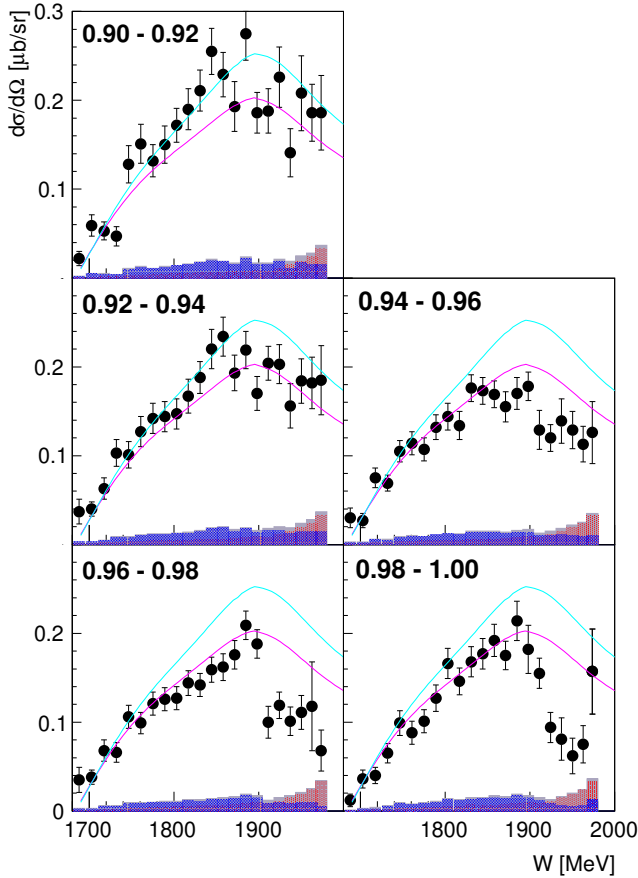


FIG. 7. $\gamma p \rightarrow K^+\Sigma^0$ differential cross section for intervals of 0.02 in $\cos \theta_{\text{CM}}^K$ (labelled inset). The labelling of data points and fits are the same as in fig. 5.

not explain the physical origin of the structure. This cusp is close to numerous thresholds of open and hidden strangeness, for example, $K^+\Lambda(1405)$, $p f_0(980)$ and $p \phi$ at 1899, 1928 and 1958 MeV respectively. The nature of the $f_0(980)$, which is often considered a $K\bar{K}$ molecular state, may support a threshold interaction. Alternatively, the cusp also appears only 50 MeV lower than the ϕN ($s\bar{s}$) threshold. Gao, Lee and Marinov [38] showed that via multiple gluon exchange, QCD equivalent Van Der Waal's forces are sufficient for bound ϕN states at the $s\bar{s}$ threshold. As was discussed in ref. [29], similar structures are evident in $K^+\Sigma^-$ and $K^+\Lambda$ excitation spectra, suggesting maybe a universal $s\bar{s}$ threshold effect.

In conclusion, differential cross sections for $\gamma p \rightarrow K^+\Sigma^0$ for $\cos \theta_{\text{CM}}^K > 0.9$ have been measured from threshold to $W = 1970$ MeV. The high statistics and $\cos \theta_{\text{CM}}^K$ resolution resolve a cusp-like structure at $W = 1900$ MeV, indicative of re-scattering effects close to multiple open and hidden strange thresholds. The Bonn-Gatchina PWA solution markedly improves the description of this data via optimising KY couplings and other parameters, which has negligible effect at more backward angles described by previous CLAS data. The tentative inclusion of a previously unobserved narrow $\Delta(1917)$ resonance, although

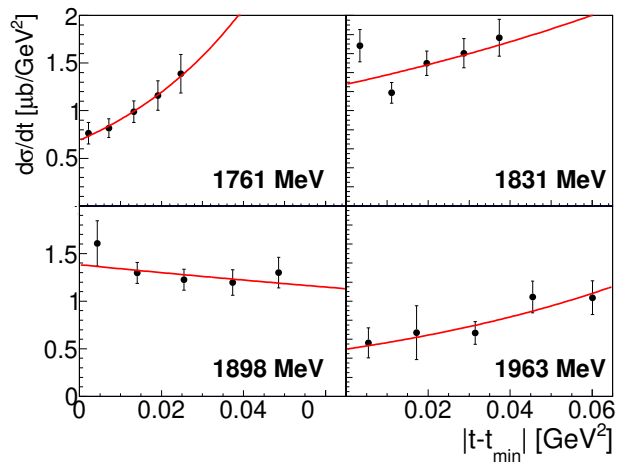


FIG. 8. $K^+\Sigma^0$ $d\sigma/dt$ versus $|t - t_{\min}|$ for intervals of centre of mass energy, W , labelled inset. Only the statistical error is shown and included in the fit. The red lines are eq. 1 fitted to the data.

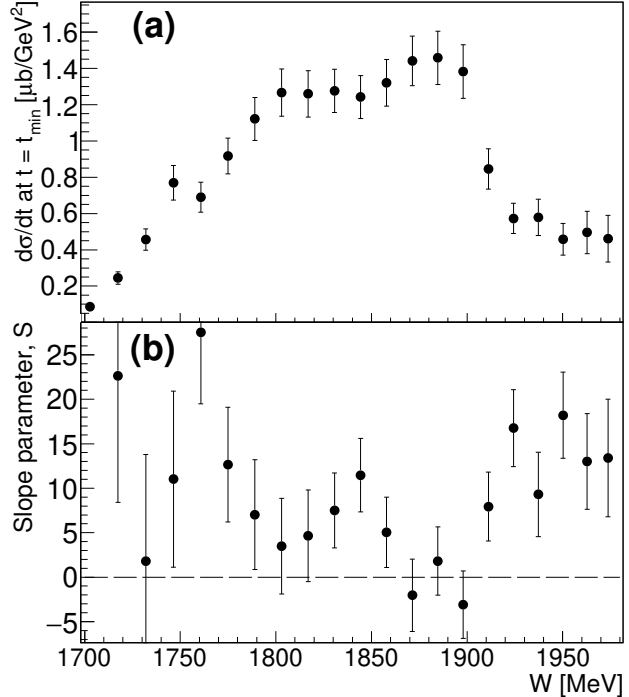


FIG. 9. (a) $K^+\Sigma^0$ differential cross section, $d\sigma/dt$ extrapolated to t_{\min} versus W . (b) The slope parameter, S versus W .

not conclusive, improves the description of the cusp-like structure and demonstrates the importance of covering this extremely forward angle range.

We would like to thank the staff and shift-students of the ELSA accelerator for providing an excellent beam. This work is supported by SFB/TR-16, DFG project numbers 388979758 and 405882627, the RSF grant number 19-42-04132, the Third Scientific Committee of the INFN

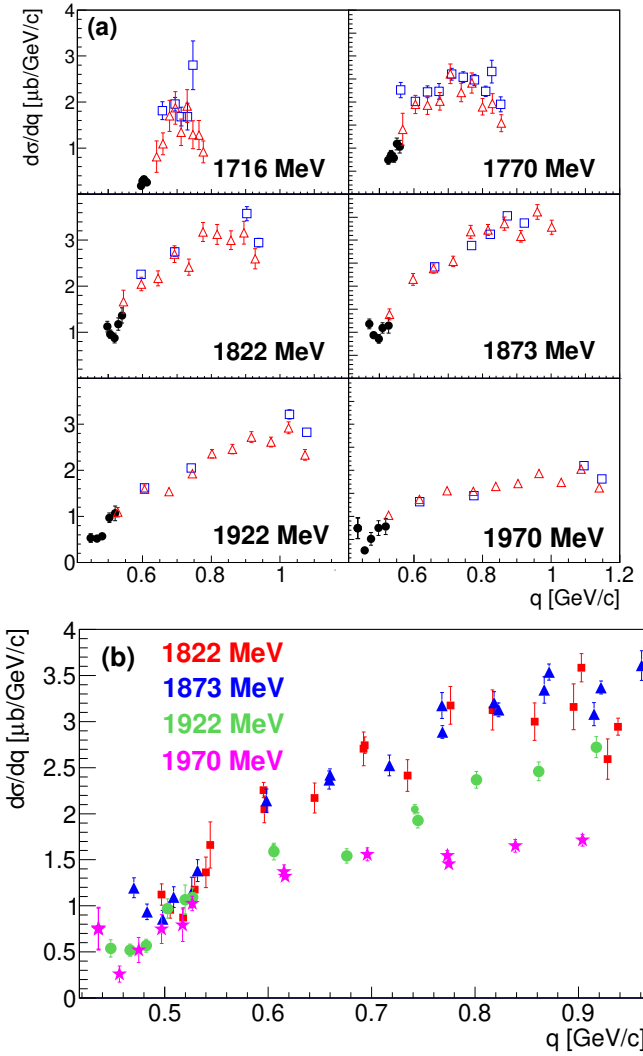


FIG. 10. $K^+\Sigma^0$ differential cross section, $d\sigma/dq$ versus three-momentum exchange, q for $\cos\theta_{\text{CM}}^K > 0.0$. (a) For different W intervals labelled inset (the nearest data point to W was used). The labelling of data points and fits are the same as in fig. 5. (b) A combination of the three data sets for the highest four W intervals (labelled). Note the smaller range in q .

and the European Unions Horizon 2020 research and innovation programme under grant agreement number 824093.

[1] R. Aaij et al. *Phys. Rev. Lett.*, 115:072001, 2015.
 [2] H. Chen, W. Chen, X. Liu, and S. Zhu. *Phys. Rep.*, 639:1, 2016.
 [3] M. Bashkanov et al. *Phys. Rev. Lett.*, 102:052301, 2009.
 [4] Gell-Mann M. *Phys. Rev. Lett.*, 8:214, 1964.
 [5] Jaffe R. L. *Phys. Rev. D*, 15:267, 1977.
 [6] D. Strottmann. *Phys. Rev. D*, (20):748, 1979.
 [7] A. Manohar and H. Georgi. *Nucl. Phys. B*, 234:189, 1984.
 [8] L. Ya. Glozman and D. O. Riska. *Physics Reports*, 268:263, 1996.
 [9] R. H. Dalitz, T. C. Wong, and G. Rajasekran. *Phys. Rev.*, 105:1617, 1967.
 [10] P. B. Siegel and W. Weise. *Phys. Rev. C*, 38:2221, 1988.
 [11] N. Kaiser, T. Waas, and W. Weise. *Nucl. Phys. A*, 612:297, 1997.
 [12] C. Garcia-Recio, M. F. M. Lutz, and J. Nieves. *Phys. Lett. B*, 582:49, 2004.
 [13] M. F. M. Lutz and E. E. Kolomeitsev. *Phys. Lett. B*, 585:243, 2004.
 [14] D. Jido, J. A. Oller, E. Oset, A. Ramos, and U. G. Meißner. *Nucl. Phys. A*, 725:181, 2003.
 [15] P. Gonzalez, E. Oset, and J. Vijande. *Phys. Rev. C*, 79:025209, 2009.
 [16] S. Sarkar et al. *Eur. Phys. J. A*, 44:431, 2010.
 [17] E. Oset and A. Ramos. *Eur. Phys. J. A*, 44:445, 2010.
 [18] R. Ewald et al. *Phys. Lett. B*, 713:180, 2012.
 [19] R. Ewald. *Phys. Lett. B*, 738:268, 2014.
 [20] E. Oset and A. Ramos. *Eur. Phys. J. A*, 44:445, 2010.

- [21] Jia-Jun Wu, R. Molina, E. Oset, and B. S. Zou. *Phys. Rev. Lett.*, 105:232001, 2010.
- [22] J. M. M. Hall et al. *Phys. Rev. Lett.*, 114:132002, 2015.
- [23] S Alef et al. *Eur. Phys. J. A*, 56:104, 2020.
- [24] W. Hillert. *Eur. Phys. J. A*, 28:139, 2006.
- [25] W. Hillert et al. *EPJ Web Conf.*, 134:05002, 2017.
- [26] S Alef et al. Submitted simultaneously to the archive. references will be updated when known. 2020.
- [27] J. Allison et al. *Nucl. Instrum. Meth. A*, 835:186, 2016.
- [28] R. Bradford et al. *Phys. Rev. C*, 81:035202, 2006.
- [29] B. Dey et al. *Phys. Rev. C*, 82:025202, 2010.
- [30] K.H. Glander et al. *Eur. Phys. J. A*, 19:251, 2004.
- [31] T. Mart and C. Bennhold. *Phys. Rev. C*, 61:012201, 1999.
- [32] S. Janssen, J. Ryckebusch, D. Debruyne, and T. Van Cauteren. *Phys. Rev. C*, 66:035202, 2002.
- [33] T. Corthals, J. Ryckebusch, and T. Van Cauteren. *Phys. Rev. C*, 73:045207, 2006.
- [34] A.V. Anisovich, V. Kleber, E. Klemp, V.A. Nikonov, A.V. Sarantsev, and U. Thoma. *Eur. Phys. J. A*, 34:243, 2007.
- [35] A. V. Anisovich et al. *Eur. Phys. J. A*, 50:129, 2014.
- [36] M. Sumihama et al. *Phys. Rev. C*, 73:035214, 2006.
- [37] S. H. Shiu, H. Kohri, et al. *Phys. Rev. C*, 97:015208, 2018.
- [38] H. Gao, T.-S. H. Lee, and V. Marinov. *Phys. Rev. C*, 63(022201(R)), 2000.